THE JOURNAL OF BIOLOGICAL CHEMISTRY
Vol. 277, No. 35, Issue of August 30, pp. 32202–32213, 2002

Printed in U.S.A.

A Model for Constitutive Lutropin Receptor Activation Based on Molecular Simulation and Engineered Mutations in Transmembrane Helices 6 and 7*

Received for publication, April 5, 2002, and in revised form, June 17, 2002
Published, JBC Papers in Press, June 17, 2002, DOI 10.1074/jbc.M203272200

Krassimira Angelova‡, Francesca Fanelli§¶, and David Puett‡‖

From the ‡Department of Biochemistry and Molecular Biology, University of Georgia, Athens, Georgia 30602-7229 and the §Department of Chemistry, University of Modena and Reggio Emilia, via Campi 183, 41100 Modena, Italy

Many naturally occurring and engineered mutations lead to constitutive activation of the G protein-coupled lutropin receptor (LHR), some of which also result in reduced ligand responsiveness. To elucidate the nature of interhelical interactions in this heptahelical receptor and changes thereof accompanying activation, we have utilized site-directed mutagenesis on transmembrane helices 6 and 7 of rat LHR to prepare and characterize a number of single, double, and triple mutants. The potent constitutively activating mutants, D556(6.44)H and D556(6.44)Q, were combined with weaker activating mutants, N593(7.45)R and N597(7.49)Q, and the loss-of-responsiveness mutant, N593(7.45)A. The engineered mutants have also been simulated using a new receptor model based on the crystal structure of rhodopsin. The results suggest that constitutive LHR activation by mutations at Asp-556(6.44) is triggered by the breakage or weakening of the interaction found in the wild type receptor between Asp-556(6.44) and Asn-593(7.45). Whereas this perturbation is unique to the activating mutations at Asp-556(6.44), common features to all of the most active LHR mutants are the breakage of the charge-reinforced H-bonding interaction between Arg-442(3.50) and Asp-542(6.30) and the increase in solvent accessibility of the cytosolic extensions of helices 3 and 6, which probably participate in the receptor-G protein interface. Asn-593(7.45) and Asn-597(7.49) also seem to be necessary for the high constitutive activities of D556(6.44)H and D556(6.44)Q and for full ligand responsiveness. The new theoretical model provides a foundation for further experimental work on the molecular mechanism(s) of receptor activation.

The superfamily of G protein-coupled receptors (GPCRs)[1] contains several members characterized by a relatively large NH_2-terminal extracellular domain responsible for high affinity binding of cognate ligands. One such member is the lutropin (luteinizing hormone) receptor (LHR) (1–3), responsible for binding the two similar gonadotropins, lutropin and hCG, that, along with the follitropin and thyrotropin hormone receptors, constitute the subfamily of glycoprotein hormone receptors (3).

At the present time, no structural data exist on the glycoprotein hormone receptors. The first crystal structure of a GPCR, bovine rhodopsin, became available in 2000 (4). Therefore, the few molecular models of the transmembrane domains of the LHR available, with or without the loops, have been constructed following *ab initio* approaches (5, 6) by using the structural information inferred from multiple alignments of GPCR sequences (7, 8) and from the electron density maps of rhodopsin (9, 10). Moreover, the finding that the extracellular domain is encoded by a series of exons, most of which yield imperfect leucine-rich repeats (1–3, 11), has led to predicted structures (12–16) based on homology modeling with ribonuclease inhibitor, a leucine-rich repeat protein of known structure (17).

A number of reports have recently appeared documenting that naturally occurring point mutations in the human LHR gene can lead to amino acid residue replacements that give rise to constitutive receptor activation and result in sporadic or familial male-limited precocious puberty (see reviews in Refs. 18–21). The most common of these is the substitution Asp-556(6.44) → Gly (the numbering system[2] in parentheses is that proposed by Ballesteros and Weinstein (Ref. 22)).

The spontaneously occurring activating mutations of the LHR have been the focus of two theoretical investigations based upon *ab initio* models of the receptor (5, 6). The LHR model by Lin *et al.* (5) suggested that single activating mutations perturb the specific interactions of TMH 6 with TMHs 5 and 7, either by disrupting the hydrophobic packing between TMHs 5 and 6 or by weakening the H-bonds between TMHs 6 and 7. That by Fanelli (6), focusing on the constitutive activation of the LHR, inferred some of the potential features characterizing the mutation-induced inactive and active LHR forms, suggesting that the active receptor states are characterized by the release of the intramolecular interactions involving the arginine of the (E/D)R(Y/W) sequence in the inactive receptor forms and by the increase in the solvent accessibility of

* This work was supported by National Institutes of Health Grant DK33973 (to D. P.) and by the Consiglio Nazionale delle Ricerche and Centro Interdipartimentale di Calcolo Automatico ed Informatica Applicata, University of Modena and Telethon-Italy Grant 68/cp (to F. F.). The costs of publication of this article were defrayed in part by the payment of page charges. This article must therefore be hereby marked "*advertisement*" in accordance with 18 U.S.C. Section 1734 solely to indicate this fact.

¶ Assistant Telethon Scientist.

‖ To whom correspondence should be addressed: Dept. of Biochemistry and Molecular Biology, B129 Life Sciences Bldg., 120 Green St., University of Georgia, Athens, GA 30602-7229. Tel.: 706-542-1676; Fax: 706-542-0182; E-mail: puett@bmb.uga.edu.

[1] The abbreviations used are: GPCR, G protein-coupled receptor; hCG, human choriogonadotropin (chorionic gonadotropin); LHR, lutropin receptor; MD, molecular dynamics; SAS, solvent-accessible surface; TMH, transmembrane helix; TSHR, thyrotropin (thyroid-stimulating hormone) receptor; WT, wild type.

[2] The numbering of human LHR generally includes the presence of the 22-amino acid residue signal peptide, whereas that of rat LHR does not. For consistency with rat LHR, we have subtracted 22 from the conventional numbering of human LHR throughout this paper. In addition to the sequential numbering, the amino acid residues in the helical bundle are labeled with numbers in parentheses indicating their relative position in the helix (22). According to this numbering system, every amino acid residue identifier starts with the helix number, followed by the position relative to a reference residue among the most conserved amino acid residue in that helix. That reference residue is arbitrarily assigned the number 50.

Trp-443(3.51) at the interface between the cytosolic extensions of TMHs 3/6 and 3/5. Although there are differences in the detailed models of the LHR TMHs (5, 6), there is general agreement that several of the TMHs, *e.g.* 3, 5, 6, and 7, participate in constitutive receptor activation.

Using site-directed mutagenesis, we and others (23, 24) have identified mutations in TMH 7 of rat and human LHR that result in constitutive receptor activation. We have also shown that, depending upon the nature of the side chain, replacements of Asn-593(7.45) and Asn-597(7.49) can result in either constitutive activation or loss-of-responsiveness, *i.e.* a subnormal response to hCG (23). TMH 7 carries a stretch of six amino acid side chains with hydrogen bonding donor and acceptor atoms: Tyr-590(7.42), Asn-593(7.45), Ser-594(7.46), Asn-597(7.49), Tyr-601(7.53), and Thr-605(7.57), all of which are localized to a common inner face of the helix. Tyr-590(7.42) belongs to a segment of TMH 7, *i.e.* 590(7.42)–592(7.44), that may adopt a non-canonical α-helix conformation. Functional roles have been ascribed to three of these residues, Asn-593(7.45), Asn-597(7.49), and Tyr-601(7.53), the last two belonging to the highly conserved NP*X*Y motif. Moreover, the results of our experiments have suggested that Asn-593(7.45) and Asn-597(7.49) are quite distinct in function, as evidenced by certain replacements that can lead to loss of function in one and gain of function in the other (23).

In view of the molecular models suggesting direct interactions between Asp-556(6.44) and asparagines 593(7.45) and 597(7.49) (5, 6, 23), as well as the experimental data demonstrating important roles of TMHs 6 and 7 in ligand-dependent and ligand-independent signaling (23–28), we have constructed and characterized a series of single, double (including reversal), and triple mutants of Asp-556(6.44) and Asn-593(7.45)/Asn-597(7.49). The feasibility of this double mutation method for LHR was initially shown by Kraaij *et al.* (29), who paired two combinations of constitutively activating mutations in human LHR, Met-376(2.43)/Met-549(6.37) and Met-376(2.43)/Asp-556(6.44), and found that the constitutive activity of the double mutant, as monitored by cAMP production in transfected HEK 293 cells, was less than that of the single mutants. Moreover, the response to hCG was blunted in the double mutants. In a preliminary communication, Kosugi *et al.* (24) prepared a double mutant of human LHR, D556(6.44)S/N597(7.49)Q, each single mutant of which was constitutively active, and also showed that the constitutive activity of the double mutant, as determined from basal cAMP levels in transfected COS-7 cells, was less than that of the single mutants. In another study, Kosugi *et al.* (30) found that double mutants of human LHR involving Asp-542(6.30), located at the cytosolic extension of TMH 6, and Asp-556(6.44) yielded mutant forms of LHR in which the basal constitutive activity was roughly additive in transfected COS-7 cells. Lack of additivity may be suggestive of a reciprocal influence of the effects exerted by two mutations, in some cases because of their spatial proximity. In contrast, additivity may be suggestive of independence of the structural effects triggered by two co-existing mutations.

By using comparative modeling and the crystal structure of rhodopsin (4) as a template, a model of the LHR has been built. Structural effects of mutations have been examined by using MD simulations and comparative analysis of average minimized structures calculated from the MD trajectories. The results of experiments and simulations reported herein with single, double, and triple mutants support the hypothesis of a direct interaction between the side chains of Asp-556(6.44) and Asn-593(7.45). The comparative analyses of the wild type and mutant receptors provide new insight into the structural rearrangements of LHR associated with mutation-induced activation.

EXPERIMENTAL PROCEDURES

Mutagenesis, Cell Culture, and Transient Transfection—Mutagenesis of the rat LHR cDNA, cloned in the expression vector pSVL, was performed by the QuikChange site-directed and *in vitro* site-directed mutagenesis kits as recommended by Stratagene and CLONTECH, respectively. Replacement of Asn-597(7.49) with Gln led to low levels of expression; this problem was overcome by using the signal sequence for hCGβ followed by its carboxyl-terminal peptide. The Sequenase version 2.0 DNA sequencing kit (Amersham Biosciences) was used to identify and verify the mutant clones. Following amplification of the mutant cDNAs, purified DNA was obtained with the Qiagen plasmid maxi kit. COS-7 cells were obtained from American Type Culture Collection and grown in a monolayer culture in Dulbecco's modified Eagle's medium supplemented with 10% (v/v) fetal bovine serum, 50 units/ml penicillin, 50 μg/ml streptomycin, 50 μg/ml gentamycin, and 0.125 μg/ml amphotericin B. The cells, maintained at 37 °C in humidified air containing 5% CO_2, were transiently transfected with 10 μg of the wild type or mutant cDNA using LipofectAMINE (Invitrogen).

Hormone Binding and cAMP Assays—Approximately 16–18 h after transfection, the cells were replated for binding (5×10^5 cells/well in six-well plates) and cAMP determinations (1×10^5 cells/well in 12-well plates), then incubated for 24 h. The incubation time for binding experiments was 16–18 h at room temperature using 50 pM ^{125}I-hCG (PerkinElmer Life Sciences), with nonspecific binding being measured in the presence of a 1,000-fold excess of hCG (CR127, kindly supplied by Dr. A. Parlow and the National Institutes of Health, Bethesda, MD). To compare the expression levels of wild type and mutant LHRs, the specific binding of wild type LHR was normalized to 100%, and the specific binding of each of the LHR mutants was given relative to that value. Competitive binding assays were used to determine IC_{50} values of WT and each mutant form of LHR based on analysis with Prism software (GraphPad Software, San Diego, CA). For the cAMP assays, cells were incubated in the presence of 0.8 mM isobutylmethylxanthine (Sigma) with medium alone (basal cAMP), increasing concentrations of hCG, and in the presence of a saturating concentration of hCG, 100 ng/ml (maximal cAMP). After removal of the medium, the cells were lysed in 100% ethanol at −20 °C overnight. The amount of cAMP in the dried extracts was measured using an ^{125}I-cAMP radioimmunoassay kit (PerkinElmer Life Sciences). EC_{50} values were obtained from the dose-response data using the Prism software. For binding and cAMP assays, duplicate determinations were made for each experiment, and the data are presented as mean ± S.E. for three to seven independent transfections. The tabulated values of basal and maximal cAMP levels are expressed as a percentage of the values corresponding to wild type LHR, each normalized to 100%. An unpaired two-tailed Student's *t* test, with 95% confidence limits, was used to establish significance ($p < 0.05$).

Building the LHR Model and Computations—The model of the human LHR employed in this work, encompassing the seven transmembrane helices and the three extracellular and three intracellular loops (sequence 359–368), was achieved by comparative modeling by means of MODELLER (31), using the crystal structure of rhodopsin as a template (4). The details of the model building have been described elsewhere.[3] Among many different input arrangements tested, a unique structure was finally selected that, following point mutations and MD simulations, produces divergent average arrangements for the inactive and active forms. For each single mutant, different starting conformations of the mutated side chain were probed by MD simulations. These conformations were assigned by using different rotamer libraries and checking for the absence of bad contacts between the mutated side chain and its neighboring amino acids. The selected conformations of the mutated side chain in the single mutants were employed in the input structures of the multiple mutants. The minimized coordinates of wild type LHR and the D542(6.30)G constitutively active mutant were used as starting points for 1,050 ps of MD runs by using CHARMM24 (32) and following the computational protocol previously described (6). Because the first 100 ps are sufficiently representative of the whole 1-ns equilibrated trajectory for all the other mutants considered in this study, 150 ps of MD run were carried out using the same heating and equilibration setup as that employed for the longer MD simulation. Finally, for the WT and all the simulated mutants, the structure averaged over the 200 structures collected (every 500 steps) during the

[3] F. Fanelli, M. Verhoef-Post, M. Timmerman, A. Zeilemaker, J. W. M. Martens, and A. P. N. Themmen, unpublished results.

TABLE I

Summary of expression and signaling parameters of individual replacements of Asp-556(6.44) (TMH 6) and Asn-593(7.45) and Asn-597(7.49) (TMH 7) in LHR

COS-7 cells were transiently transfected with wild type and mutant cDNAs to LHR and characterized by specific binding of ^{125}I-hCG and cAMP production, both basal and stimulated (Max.) in the presence of hCG (100 ng/ml). Mean values for B_o, basal cAMP, and hCG-stimulated cAMP for wild type LHR were 12,467 ± 1,240 cpm, 2.6 ± 0.2 pmol/ml, and 48 ± 4 pmol/ml (n = 26), respectively, and these parameters are presented as a percentage of wild type LHR controls. IC_{50} and EC_{50} values were determined from competitive binding and hCG-mediated cAMP increases, respectively; these parameters are in nM. ND, not determined. Asp-556, Asn-593, and Asn-597 correspond to residues (6.44), (7.45), and (7.49), respectively.

LHR	B_o	IC_{50}	Basal cAMP	EC_{50}	Max. cAMP
	%	nM	%	nM	%
WT LHR	100	0.2 ± 0.06	100	0.2 ± 0.04	100
n	26	13	26	13	26
D556H[a]	117 ± 13	0.1 ± 0.01	**1,443 ± 307**[b]	0.1 ± 0.08	79 ± 9
n	10	2	10	2	10
D556Q[a]	127 ± 26	0.1 ± 0.06	**1,023 ± 488**[b]	0.4 ± 0.3	110 ± 31
n	5	2	5	2	5
D556A[a]	15 ± 2[b,c]	0.4 ± 0.1	**196 ± 28**[b,c]	0.4 ± 0.01	22 ± 4[b,c,d]
n	5	3	5	3	5
D556N	157 ± 19	0.1 ± 0.08	120 ± 9	0.1 + 0.02	139 ± 26
n	6	2	6	2	6
N593R[a]	187 ± 57[e]	0.6 ± 0.4	**261 ± 37**[e]	0.2 ± 0.03	80 ± 18[e]
n	5	2	5	2	5
N597Q[a]	94 ± 4[e]	0.1 ± 0.02	**160 ± 9**[e]	0.1 ± 0.01	99 ± 4[e]
n	4	2	4	2	4

[a] Mutants that represent constitutive receptor activation are indicated in bold type.
[b] Significantly different from wild type LHR.
[c] From Ref. 34 (IC_{50} and EC_{50} values were, however, not available in that preliminary communication and were determined in this study).
[d] The reduced responsiveness to hCG may result from the relatively low expression.
[e] From Ref. 23 (IC_{50} and EC_{50} values were not available in the earlier report and were determined in this study).

50,500–150,000-step interval and minimized were used for the comparative analysis.

RESULTS

Engineered Mutations in TMHs 6 and 7 of LHR—A number of replacements of Asp-556(6.44) in human and rat LHR have been characterized, some of these representing naturally occurring mutations in human LHR and others engineered mutations in both human and rat LHR. Those substitutions yielding constitutively activated receptor include Gly, Glu, Ser, Leu, Phe, Tyr, and His (26, 33), with His giving the greatest degree of activation. Of the replacements investigated, only Asn gave a phenotype like that of wild type LHR, whereas the introduction of Pro interfered with expression (26). In support of these results with human LHR, we found that the D556(6.44)H increased the basal cAMP level to 1,443 + 307%, whereas D556(6.44)N did not significantly affect the basal cAMP level in COS-7 cells expressing comparable numbers of mutant and wild type receptors (Table I). We also reported elsewhere that the D556(6.44)A mutant is constitutively active even at a low receptor density, although IC_{50} and EC_{50} values were not available in that study (34). The IC_{50} and EC_{50} values of the D556(6.44)H,Q,A,N LHR mutants, along with other pertinent parameters, are given in Table I; those for D556(6.44)H,Q,N do not differ significantly from that of wild type LHR, nor do the maximal levels of hCG-stimulated cAMP production. LHR functionality, as determined by basal and hCG-stimulated cAMP production, was dependent to some extent on receptor density. For example, the basal cAMP level associated with the most potent constitutively activated mutation yet examined, D556(6.44)H, increased with increasing receptor density, whereas that for wild type LHR did not. In contrast, the maximal amount of cAMP produced in response to a saturating concentration of hCG was dependent on receptor levels for the wild type and D556(6.44)H mutant LHRs (data not shown). Thus, whenever possible, comparisons are made with cells expressing comparable levels of wild type and mutant LHRs.

Earlier we determined that the N593(7.45)R and N597(7.49)Q mutants of rat LHR were constitutively active and responsive to ligand (23), and the results in Table I show that their hCG affinity, potency, and efficacy in hCG-stimulated cAMP production are comparable with that of wild type LHR. We also observed that the N593(7.45)A mutant exhibited a partial loss of responsiveness to ligand, whereas the N593(7.45)D and N597(7.49)D mutants expressed poorly (23). To experimentally probe possible interhelical interactions between TMHs 6 and 7, a number of double mutants were made to test the hypothesis that Asp-556(6.44) interacts with Asn-593(7.45) and/or Asn-597(7.49) (5, 6, 23, 24, 34). The combinations were chosen to pair two point mutants, one in each TMH, that alone represented either a constitutively active or a loss-of-responsiveness mutant. Another question being asked was, what is the dominant phenotype in a double mutant in which the individual replacements exhibit opposite effects?

We first investigated double mutants containing the most potent activating mutant known, His-556(6.44) (33), and either the loss-of-responsiveness mutant, Ala-593(7.45), or the weak constitutively active mutants, Arg-593(7.45) and Gln-597(7.49) (23). As shown in Table II, only the double mutants D556(6.44)H/N593(7.45)A and D556(6.44)H/N597(7.49)Q exhibited constitutive activity, albeit with reduced levels of basal cAMP production (462 + 112% and 335 + 52%, respectively) compared with the D556(6.44)H mutant (1,443 + 307%). The two activating point mutants, D556(6.44)H and N593(7.45)R, when combined (D556(6.44)H/N593(7.45)R) gave a somewhat elevated, but not significantly so, basal cAMP level (186 + 35%). Pairing the other potent constitutively activating mutant, Gln-556(6.44), with either one of the weaker activating mutants, Arg-593(7.45) and Gln-597(7.49), resulted in double mutants that were not constitutively active (Table II). These five LHR double mutants exhibited IC_{50} values comparable with that of wild type LHR; the efficacy of hCG-stimulated cAMP production was reduced in the D556(6.44)H/N593(7.45)A, D556(6.44)H/N593(7.45)R, and D556(6.44)Q/N593(7.45)R mutants. The reduced efficacy of the D556(6.44)H/N593(7.45)R and D556(6.44)Q/N593(7.45)R mutants prevented an accurate determination of their EC_{50} values, which for the others were like that of wild type LHR.

Two reversal mutants, D556(6.44)N/N593(7.45)D and D556(6.44)N/N597(7.49)D, were then prepared to test more

TABLE II

Summary of the expression and signaling parameters of double and triple mutants of LHR involving replacements of Asp-556(6.44) (TMH 6) and Asn-593(7.45) and Asn-597(7.49) (TMH 7)

Transiently transfected COS-7 cells were assayed for specific binding of ^{125}I-hCG and for cAMP production, both basal and hCG-stimulated (100 ng/ml) (Max.). Mean values of B_o, basal cAMP, and hCG-stimulated cAMP for wild type LHR were 13,891 ± 1,406 cpm, 2.4 ± 0.2 pmol/ml, and 51 ± 15 pmol/ml (n = 22), respectively, these values being presented as a percentage of the wild type LHR controls. The IC_{50} and EC_{50} values were determined from competitive binding and hCG-mediated increases in cAMP production, respectively, and are given in nM. Asp-556, Asn-593, and Asn-597 correspond to residues (6.44), (7.45), and (7.49), respectively.

LHR	B_o	IC_{50}	Basal cAMP	EC_{50}	Max. cAMP
	%	nM	%	nM	%
His-556-containing double mutants					
D556H/N593A[a]	208 ± 35	0.3 ± 0.07	**462 ± 112**[b]	0.2 ± 0.1	52 ± 10[b]
n	4	2	4	2	4
D556H/N597Q[a]	140 ± 32	0.2 ± 0.1	**335 ± 52**[b]	0.1 ± 0.02	80 ± 16
n	4	2	4	2	4
D556H/N593R	147 ± 36	0.4 ± 0.05	186 ± 35	—[c]	13 ± 4[b]
n	4	2	4	2	4
Gln-556-containing double mutants					
D556Q/N593R	209 ± 52	0.2 ± 0.05	129 ± 23	—[c]	25 ± 8[b]
n	4	2	4	2	4
D556Q/N597Q	138 ± 19	0.2 ± 0.04	134 ± 22	0.2 ± 0.07	53 ± 10
n	4	2	4	2	4
Asn-556-containing (reversal) double mutants					
D556N/N593D	23 ± 2[b]	0.1 ± 0.05	96 ± 12	0.2 ± 0.03	61 ± 11
n	6	2	6	2	6
D556N/N597D	51 ± 2[b]	0.1 ± 0.03	81 ± 10	0.2 ± 0.03	59 ± 7[b]
n	5	2	5	2	5
Triple mutants					
D556H/N593A/N597A	277 ± 87	0.1 ± 0.01	86 ± 9	—[c]	—[d]
n	4	2	4	2	4
D556N/N593A/N597A	84 ± 28	0.2 ± 0.1	84 ± 6	—[c]	—[d]
n	4	2	4	2	4

[a] Constitutively activating mutants are indicated in bold type.
[b] Significantly different from wild type LHR.
[c] Ligand-mediated signaling was too low to obtain a meaningful EC_{50}.
[d] The triple mutants were non-responsive to hCG; the cAMP values in the presence of ligand were not significantly different from the basal cAMP levels.

directly the putative interaction between TMHs 6 and 7. As shown in Table II, these reversal mutants express at levels somewhat lower than wild type LHR, but there is no evidence of constitutive activity in either. Although the lower expression level may mask constitutive activation, we do not believe this to be the case because constitutive activity was noted in the D556(6.44)A mutant, which expressed at a lower level than either of the reversal mutants. These two reversal mutants exhibited IC_{50} and EC_{50} values like those of wild type LHR; only the D556(6.44)N/N597(7.49)D mutant exhibited a marginal reduction in efficacy of hCG-stimulated cAMP production.

Next, two triple mutants of LHR, D556(6.44)N/N593(7.45)A/N597(7.49)A and D556(6.44)H/N593(7.45)A/N597(7.49)A, were constructed and characterized. They expressed well, especially the D556(6.44)H/N593(7.45)A/N597(7.49)A mutant, and had basal cAMP and IC_{50} values like those of wild type LHR. Interestingly, neither of the triple mutants was constitutively active nor responsive to hCG (Fig. 1 and Table II).

Additivity Versus Synergy in Double Mutants of LHR—In an effort to better compare the responsiveness of double LHR mutants relative to results obtained with the constitutively active single mutants, we have calculated the expected values of basal cAMP based on additivity of the two single mutants and compared these parameters with the experimental measurements (Table III). Results are included only for those single and double mutants that expressed at levels comparable with that of wild type LHR. The difference between the experimentally determined parameters of the double mutants and the values expected from additivity of the two appropriate single mutants is a measure of the deviation from additivity and can thus reflect synergy or, in molecular terms, direct *versus* indirect effects of interacting side chains.

Interestingly, the Δ(basal cAMP) values for the double mutants of rat LHR, D556(6.44)H/N593(7.45)A, D556(6.44)H/N597(7.49)Q, D556(6.44)H/N593(7.45)R, D556(6.44)Q/N593(7.45)R, and D556(6.44)Q/N597(7.49)Q, are not significantly different one from another and average −(31 ± 6) pmol/ml, *i.e.* replacement of Asn-593(7.45) with Ala or Arg, or of Asn-597(7.49) with Gln, reduces the level of constitutive activation associated with D556(6.44)H and D556(6.44)Q by a fairly constant amount. We have also used this approach to analyze the results of Kosugi *et al.* (30), who prepared double mutants of human LHR with the same Asp in TMH 6, *i.e.* Asp-556(6.44), and Asp-542(6.30) in intracellular loop 3. As shown in Table III, the basal cAMP values of the double mutants, D542(6.30)N/D556(6.44)G and D542(6.30)N/D556(6.44)S, are, within experimental error, predictable from the properties of the constituent single mutants; only D542(6.30)N/D556(6.44)Y appears to deviate somewhat from additivity.

Computer Simulations on a Novel LHR Model: Structural Features of Wild Type LHR—Very recently, the crystal structure of rhodopsin became available (4). Therefore, we have built another LHR model based on the human sequence by using the rhodopsin structure as a template. The comparative modeling of LHR, as well as the differences between the previous *ab initio* model (6) and the recent homology model of human LHR, have been described elsewhere.[3] In this work, we have employed only the homology model because of the probable higher reliability of the seven-TMH architecture as compared with the *ab initio* model.

MD simulations have been done on all of the single and multiple mutants considered in this work as well as on natural and engineered mutants from the literature (18–21, 26, 30). The comparative analysis of the average minimized structures obtained from MD trajectories of wild type LHR and its mutants has revealed novel structural features of the active and

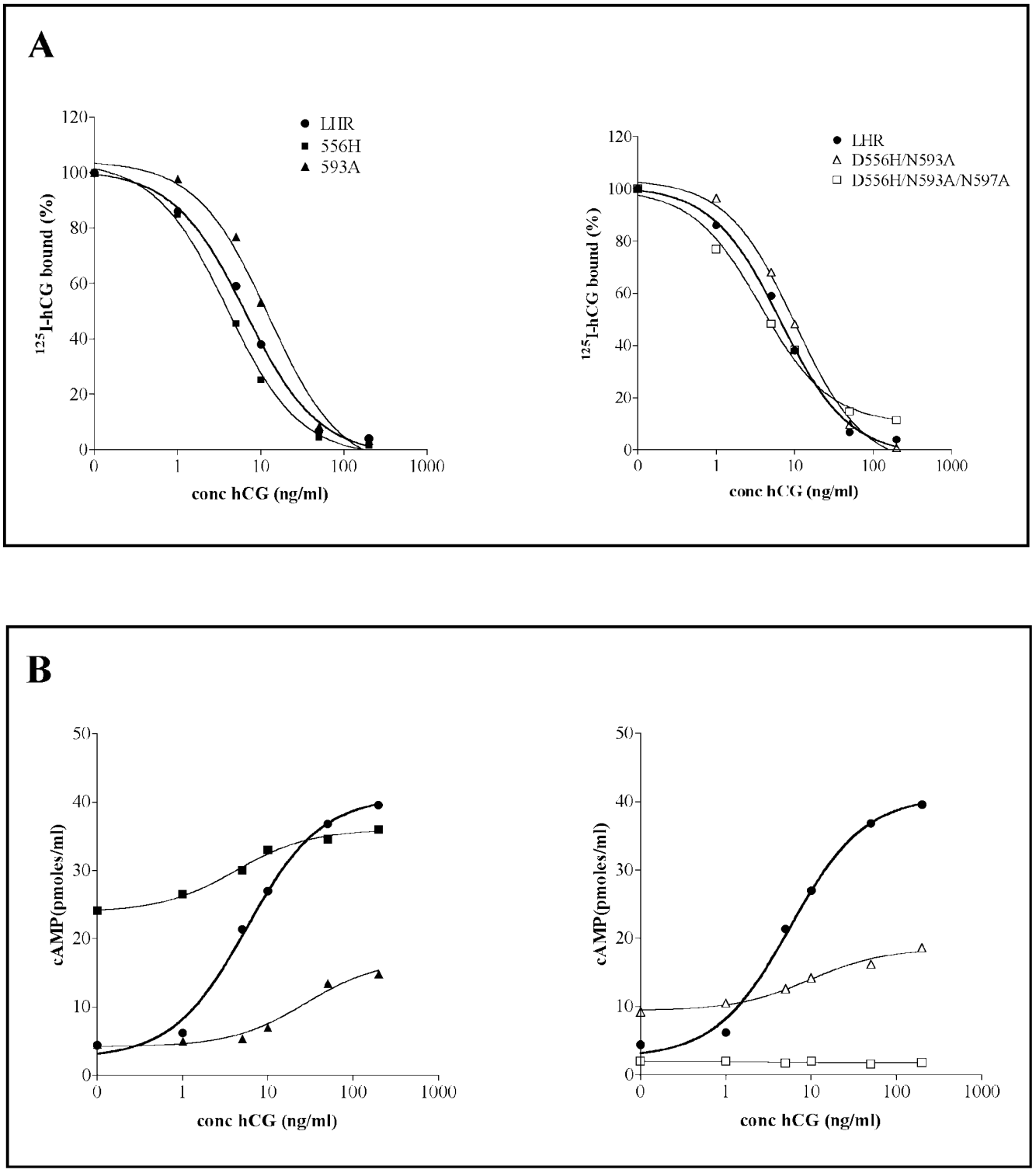

FIG. 1. **Representative competition binding curves (^{125}I-hCG and hCG) and hCG-mediated cAMP production for wild type LHR, D556(6.44)H, N593(7.45)A, D556(6.44)H/N593(7.45)A, and D556(6.44)H/N593(7.45)A/N597(7.49)A.** Competitive binding results are presented in the upper panels, A and B, and the cAMP changes in response to hCG are given in panel C.

inactive forms that have been interpreted in the context of the experimental mutagenesis data. The limited amino acid sequence differences between rat and human LHR are believed to be of no significant consequence in comparing the experimental and modeling results. This assumption is also supported by the finding that mutations of Asp-556(6.44) to His and Asn produce similar functional effects of LHR in the two different species.

Similarly to the *ab initio* model (6), the LHR sites susceptible to activating mutations in the homology model are interhelical positions close to highly conserved amino acid residues. In particular, in wild type LHR, Asp-556(6.44), the amino acid residue extensively targeted in this study, is engaged in H-bonding interaction with the highly conserved Asn-593(7.45). This interaction had been previously proposed based upon the model of human LHR built by Lin *et al.* (5), which suggested a double H-bonding interaction between Asp-578(6.44) (corre-

TABLE III

Comparison of additivity and synergy principles reflected in constitutive activation of LHR double mutants

COS-7 cells were transiently transfected with wild type and mutant cDNAs to LHR and characterized by basal cAMP (bcAMP) levels. Exp refers to the experimentally determined parameters for the double mutant minus that for wild type LHR; Add denotes the expected value base on additivity of the two consistent single mutants, each minus that for wild type LHR. Data are included only for those single and double LHR mutants that expressed at levels comparable with wild type LHR. Asp-542, Asp-556, Asn-593, and Asn-597 correspond to residues (6.30), (6.44), (7.45), and (7.49), respectively.

Double mutant	bcAMP (Exp)	bcAMP (Add)	Δ(bcAMP) (Exp-Add)
D556H/N593A[a]	9.4 ± 1.1	35.1 ± 3.2	−25.7 ± 3.4
D556H/N597Q[a]	6.1 ± 0.6	36.5 ± 3.1	−30.4 ± 3.2
D556H/N593R[a]	2.2 ± 0.4	39.1 ± 3.1	−36.9 ± 3.1
D556Q/N593R[a]	0.8 ± 0.3	28.2 ± 3.1	−27.4 ± 3.1
D556Q/N597Q[a]	0.9 ± 0.3	25.6 ± 3.1	−24.7 ± 3.1
D542N/D556G[b]	8.9 ± 0.6	8.9 ± 0.7	0 ± 0.9
D542N/D556S[b]	12.7 ± 0.6	9.4 ± 0.5	+3.3 ± 0.8
D542N/D556Y[b]	11.7 ± 0.7	14.2 ± 0.8	−2.5 ± 1.1

[a] The experimentally determined values for basal cAMP levels (pmol/ml) of cells expressing rat LHR are from Tables I and II, with the exception of the data for N593A that were taken from Ref. 23.

[b] The experimentally determined values for basal and maximal cAMP levels (pmol/10^5 cells) of cells expressing human LHR are from Table I of Ref. 30. (The numbering used in the table is based on the receptor without the signal peptide; the standard convention for human LHR would list these two amino acid residues as Asp-564 and Asp-578).

sponding to Asp-556(6.44) in rat LHR) and both the conserved asparagines Asn-615(7.45) and Asn-619(7.49) (corresponding, respectively, to Asn-593(7.45) and Asn-597(7.49) in rat LHR). Our simulations suggest the Asp-556(6.44)-Asn-593(7.45) interaction as highly probable, whereas the Asp-556(6.44)-Asn-597(7.49) interaction seems to be unlikely. Our simulations, however, do not exclude an interaction of Asp-556(6.44) with Asn-597(7.49) via a water molecule (34). These results are suggestive of a structural difference between Asn-593(7.45) and Asn-597(7.49), consistent with the experimental findings that they are quite distinct in function (23).

In wild type LHR, the highly conserved polar amino acids, Asn-355(1.50), Asp-383(2.50), and Asn-597(7.49), as well as Asn-593(7.45) and Ser-594(7.46), cluster far away from the arginine of the (E/D)R(Y/W) sequence, being interconnected by a network of H-bonding interactions (Fig. 2). In particular, Asp-383(2.50) interacts with both Asn-355(1.50) and Ser-594(7.46), linking TMH 2 with both TMHs 1 and 7; Asn-593(7.45) interacts with both Ser-431(3.39) and Asp-556(6.44) linking TMH 7 with both TMHs 3 and 6; whereas Asn-597(7.49) interacts with both Asn-355(1.50) and Lys-548(6.36), linking TMH 7 with both TMHs 1 and 6 (Fig. 2). These interactions highlight the structural importance of the cytosolic half of TMH 7. In fact, this portion of the receptor has the majority of the polar amino acid residues that make H-bonding connections between this helix and all the TMHs 1, 2, 3, and 6 (Fig. 2). It is noteworthy that, in the wild type structure averaged over all the 2,000 structures collected during the 1-ns trajectory, Tyr-590(7.42) substitutes for Asn-593(7.45) as an interacting partner of Ser-431(3.39), whereas Asn-597(7.49) loses its interaction with Asn-355(1.50) found in the early steps of simulation. In contrast, all of the other interactions involving the polar residues in TMHs 1, 2, 3, and 7 in the first 100 ps are almost persistent during the entire 1-ns time of simulation.

Another important feature of the wild type structure is the charge reinforced H-bonding interaction between Arg-442(3.50), the arginine of the (E/D)R(Y/W) sequence, and both the adjacent glutamate, Glu-441(3.49), and Asp-542(6.30) in the cytosolic extension of TMH 6 (Fig. 2). This interaction is persistent over the complete 1-ns MD trajectory. A similar interaction pattern is found in the rhodopsin structure between Arg-135(3.50) and both Glu-134(3.49) and Glu-247(6.30). On the other hand, Asp-542(6.30) is also involved in a salt bridge interaction with the adjacent Lys-541(6.29).

In summary, in the wild type LHR, a network of H-bonds involving the highly conserved amino acid residues in the cytosolic halves of TMHs 1, 2, 3, and 7 is associated with a charge-reinforced H-bonding interaction in the cytosolic domains between the arginine of the (E/D)R(Y/W) motif and Asp-542(6.30). This interaction links together the cytosolic extensions of TMHs 3 and 6.

Computer Simulations of Asp-556(6.44), Asn-593(7.45), and Asn-597(7.49) Mutations: Structural Perturbations in Proximity to the Mutated Positions—In general, all the different replacements of Asp-556(6.44) considered in this work perturb the interaction found in the WT LHR between the replacing amino acid residue and Asn-593(7.45). Perturbations include the breakage of the Asp-556(6.44)-Asn-593(7.45) H-bonding interaction as induced by mutations of Asp-556(6.44) to Ala, Gly, Leu, His, and Tyr (Figs. 3 and 4). In the D556(6.44)Y mutant and, to a lesser extent in the D556(6.44)L mutant, van der Waals interactions between positions 556(6.44) and 593(7.45) substitute for the H-bonding interaction found in wild type LHR. In the highly active mutants D556(6.44)H,Y,G, the loss of the H-bonding interaction between Asp-556(6.44) and Asn-593(7.45) is associated with the gain of a new H-bonding interaction between Asn-593(7.45) and the highly conserved Asp-383(2.50) in TMH 2. In the D556(6.44)Q constitutively active mutant, the Gln substituting for Asp-556(6.44) still performs H-bonding with Asn-593(7.45), although with a different geometry as compared with the wild type receptor. Replacement of Asp-556(6.44) with Asn, or a combination of the D556(6.44)N with the N593(7.45)D mutant, shows a propensity to conserve the H-bonding interaction found in the wild type LHR between the amino acids in positions 556(6.44) and 593(7.45). Perturbations of the Asp-556(6.44)-Asn-593(7.45) interaction are associated with rearrangements in the network of H-bonding interactions involving, in the wild type receptor, the polar amino acids in TMHs 1, 2, 3, and 7.

This rearrangement is essentially the result of the majority of these polar amino acids lying in a portion of TMH 7, *i.e.* from Tyr-590(7.42) to Tyr-601(7.53) characterized by high mobility, essentially the result of the presence of two prolines, near the beginning and ending of this segment, *i.e.* Pro-591(7.43) and Pro-598(7.50). Indeed, Pro-591(7.43) belongs to the 590(7.42)–592(7.44) segment that frequently deviates from the α-helix conformation. Perturbations in the interactions of the polar amino acids are also caused by mutations of Asn-593(7.45) and Asn-597(7.49) to Arg and Gln, respectively, as well as by Ala replacements of the two asparagines. In particular, the N593(7.45)R mutant is characterized by a salt bridge between the replacing Arg and both Asp-383(2.50) and Asp-556(6.44).

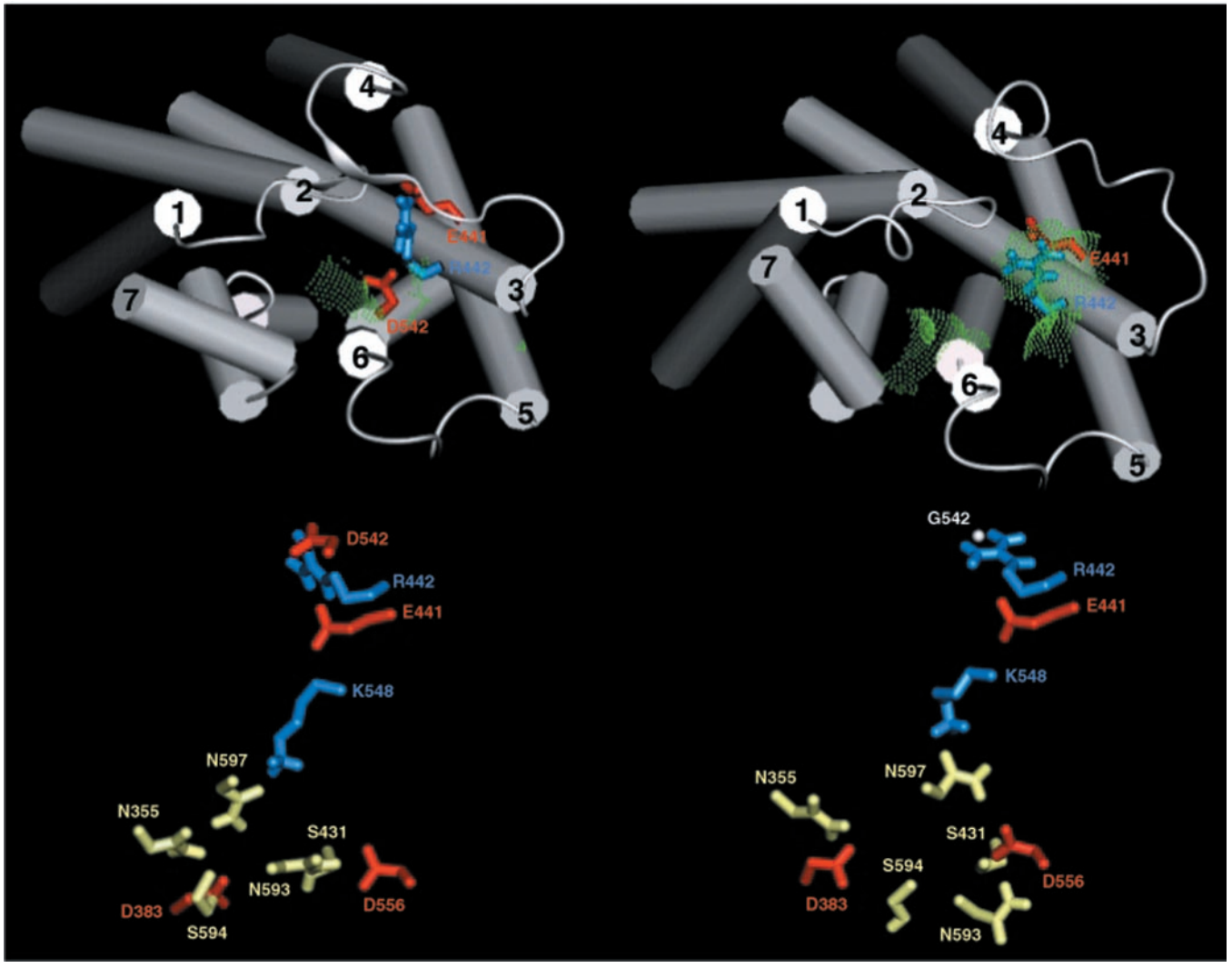

FIG. 2. **Average minimized structures of wild type LHR (*top* and *bottom left*) and the D542(6.30)G constitutively activating mutant (*top* and *bottom right*).** In the *top panel*, the helix bundles are represented by *cylinders* whereas the three intracellular loops are represented by *thin ribbons*. The extracellular domains are not shown in this figure. The structures are viewed from the intracellular side in a direction almost perpendicular to the membrane surface. The side chains of Glu-441(3.49), Arg-442(3.50), Asp-542(6.30), and Gly-542(6.30) are represented by *sticks* and *colored* according to their polarity. The composite solvent-accessible surface computed over the amino acids Arg-442(3.50), Thr-445(3.53), Ile-446(3.54), and Lys-541(6.29) is also shown, represented by *green dots*. In particular, SAS is 28 Å^2 in the wild type and 120 Å^2 in the D542(6.30)G active mutant. In the *bottom panel*, details of the interactions of the arginine and glutamate of the ERW motif, as well as of the polar conserved amino acids, are shown. The amino acid side chains, which are colored according to their polarity, are seen in a direction almost parallel to the membrane surface.

Computer Simulations on the LHR Mutants: Structural Perturbations in the Cytosolic Domains—The homology model suggests that Asp-542(6.30) contributes to stabilize the inactive state of the LHR through a salt bridge with the arginine of the (E/D)R(Y/W) sequence. Simulations of the D542G constitutively active mutant show that the breakage of the Arg-442(3.50)-Asp-542(6.30) charge-reinforced H-bonding interaction favors the solvent exposure of amino acid residues at the cytosolic extensions of TMHs 3 and 6, including the arginine of the (E/D)R(Y/W) motif (Fig. 2). The augmented solvent accessibility of these receptor portions, as compared with the wild type receptor, is properly described by the solvent-accessible surface area computed over amino acid residues Arg-442(3.50), Thr-445(3.53), Ile-446(3.54), and Lys-541(6.29) (SAS represented by *green dots* in Fig. 2). In fact, considering the structures averaged over the 200 collected during the first 100 ps of the 1-ns trajectory and minimized, this index is 28 Å^2 in the wild type LHR, whereas it is 120 Å^2 in the D542(6.30)G active mutant. The SAS index remains, respectively, below and above those values during the complete 1-ns time of simulation of wild type LHR and the D542(6.30)G constitutively active mutant.

Simulations of the known spontaneously occurring activating and inactivating mutations of LHR have shown that SAS is indeed a good marker of the functional receptor state, being less than 50 Å^2 in non-constitutively active mutants and above this threshold in the constitutively active mutants.[3]

Additionally, the D542(6.30)N mutant simulated in this work displays a SAS value above the threshold, consistent with the experimental findings that it is constitutively active (30) (Fig. 3). In this mutant, a weak H-bonding interaction between Arg-442(3.50) and Asn-542(6.30) can be formed, even if not persistently during the simulation time.

Simulations of the Asp-556(6.44) mutants from the literature (26), as well as of the LHR mutants engineered in this work, strengthen the ability of SAS to differentiate the active from the inactive forms (Table IV). In fact, mutations of Asp-556(6.44) to Ala, Gly, His, Gln, Tyr, and Leu, which increase the basal activity of LHR, are characterized by an increase of SAS above the threshold (Table IV, Fig. 3), as well as by the

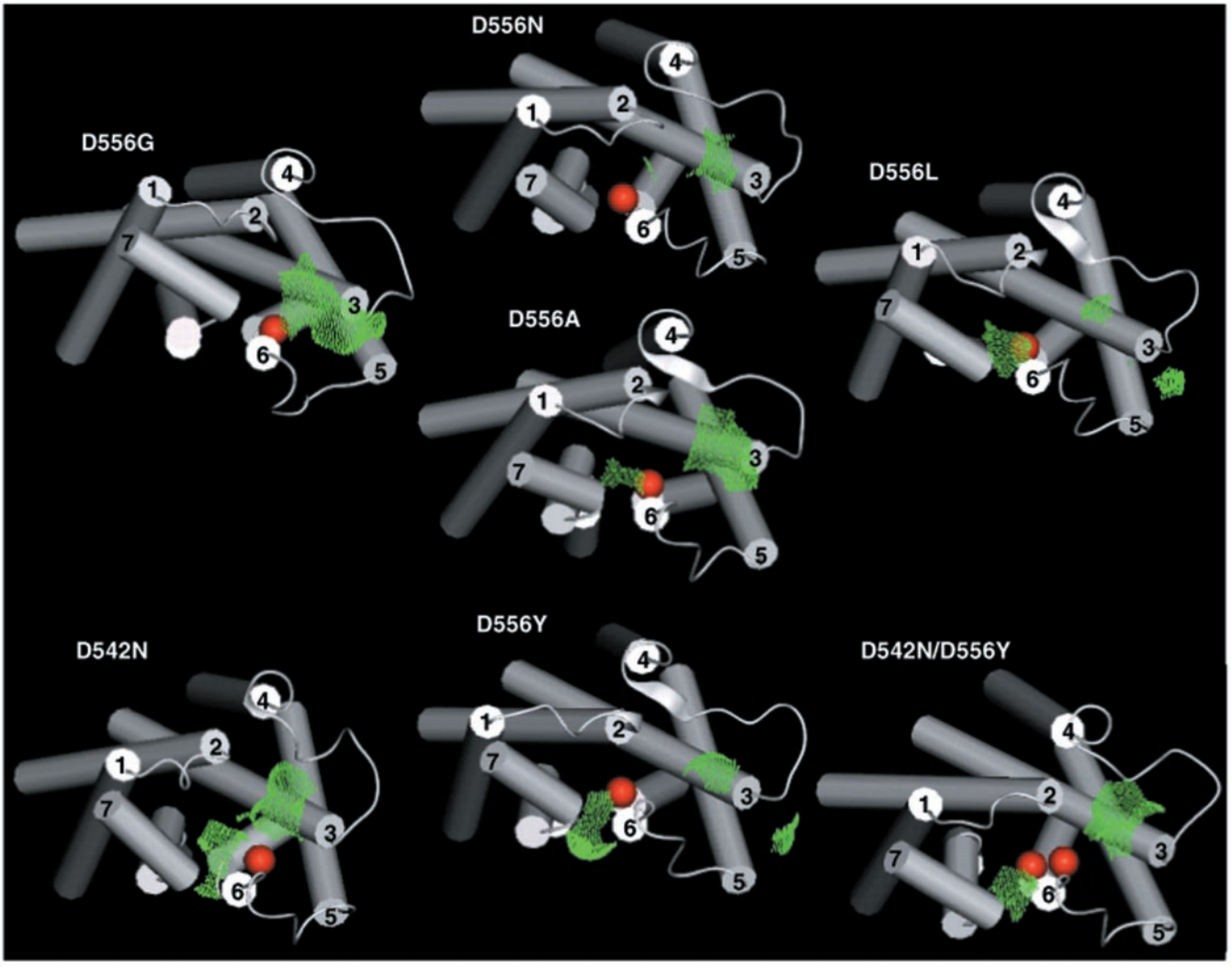

FIG. 3. **Average minimized structures of wild type LHR and the mutants D556(6.44)N, D556(6.44)G, D556(6.44)A, D556(6.44)L, D556(6.44)Y, D542(6.30)N, and D542(6.30)N/D556(6.44)Y.** The structures are viewed from the intracellular side in a direction almost perpendicular to the membrane surface. The extracellular domains are not shown in this figure. Each mutated position is indicated by a *red sphere*. The composite solvent-accessible surface computed over the amino acids Arg-442(3.50), Thr-445(3.53), Ile-446(3.54), and Lys-541(6.29) is also shown, represented by *green dots*.

breakage of the charge-reinforced H-bonding interaction found in wild type LHR between Arg-442(3.50) and Asp-542(6.30). On the other hand, the D556(6.44)N non-constitutively active mutant is characterized by the presence of both the Glu-441(3.49)-Arg-442(3.50) and Arg-442(3.50)-Asp-542(6.30) interactions found in the wild type receptor and by SAS below the threshold, features of the inactive forms. Thus, in the active mutants of Asp-556(6.44), perturbations in the H-bonding interaction found in wild type LHR between Asp-556(6.44) and Asn-593(7.45) are associated with structural perturbations in the cytosolic extensions of TMHs 3 and 6, *i.e.* the breakage of a charge-reinforced H-bonding interaction between Arg-442(3.50) and Asp-542(6.30), as well as an increase in the solvent accessibility of selected amino acids including Arg-442(3.50) (Table IV).

In contrast, in the constitutively active mutants of Asp-542, perturbations in the arrangements of the cytosolic ends of TMHs 3 and 6 are not associated with the breakage of the Asp-556(6.44)-Asn-593(7.45) interaction. In other words, activating mutations of Asp-556(6.44) exert a strong influence on the interaction pattern of Asp-542(6.30), whereas activating mutations of Asp-542(6.30) do not significantly perturb the interactions of Asp-556(6.44). In line with these suggestions, some of the structural features of the D556(6.44)Y mutant (including the interaction patterns of Asp-383(2.50), Asn-593(7.45), and Asn-597(7.49), the breakage of the Arg-442(3.50)-Asp-542(6.30) interaction, and the arrangement of the cytosolic domains) are almost conserved in the average minimized structure of the double D542(6.30)N/D556(6.44)Y mutant, prevailing over those of the D542(6.30)N mutant (Fig. 3). These results also suggest that the constitutive activity of the D542(6.30)N/D556(6.44)Y double mutant is almost entirely the result of the structural effects of the Asp-556(6.44) mutation, consistent with the similarity between their basal activities (30). According to both the SAS index (91 $Å^2$) and the interaction pattern of Arg-442(3.50), the D542(6.30)N/D556(6.44)Y mutant is correctly predicted to be constitutively active (Fig. 3).

On the other hand, predictions of the functional behavior of the N593(7.45)R mutant gives ambiguous results. In fact, the selected average structure is characterized by the lack of the Arg-442(3.50)-Asp-542(6.30) interaction, a feature of the active forms, but is associated with a SAS value below the threshold, a feature of the inactive ones (Fig. 4). Thus, the N593(7.45)R mutant exhibits some features of the active forms and some others of the inactive ones. Thus, computer simulations predict

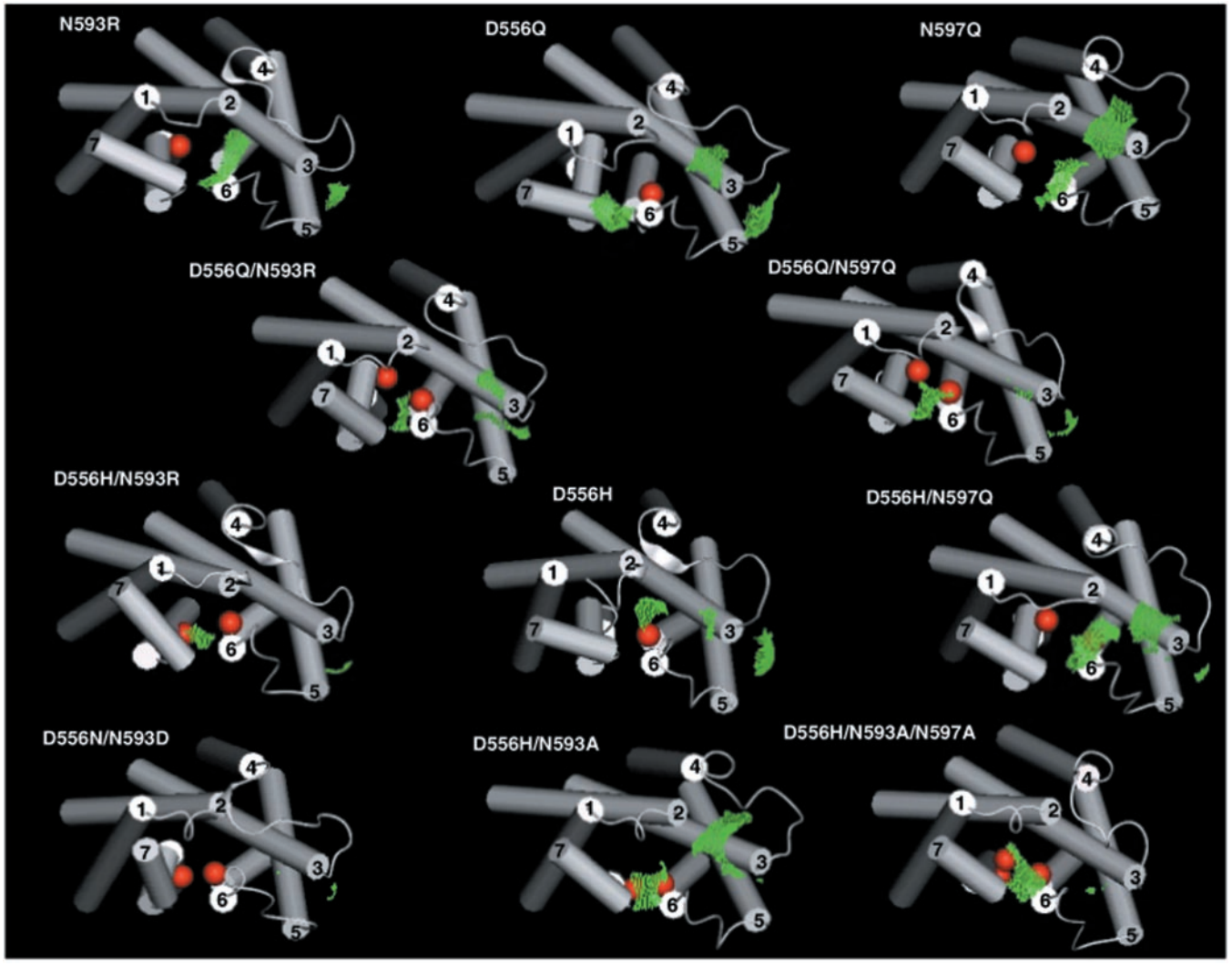

FIG. 4. **Average minimized structures of the N593(7.45)R, D556(6.44)Q, N597(7.49)Q, D556(6.44)Q/N593(7.45)R, D556(6.44)Q/N597(7.49)Q, D556(6.44)H, D556(6.44)H/N593(7.45)R, D556(6.44)H/N597(7.49)Q, D556(6.44)N/N593(7.45)D, D556(6.44)H/N593(7.45)A, and D556(6.44)H/N593(7.45)A/N597(7.49)A LHR mutants.** The structures are viewed from the intracellular side in a direction nearly perpendicular to the membrane surface, and the extracellular domains are not shown. Each mutated position is indicated by a *red sphere*. The composite solvent-accessible surface area computed over the amino acids Arg-442(3.50), Thr-445(3.53), Ile-446(3.54), and Lys-541(6.29) is also shown, represented by *green dots*.

the N593(7.45)R mutant as weakly active or even non-constitutively active.

Pairing the constitutively active mutant D556(6.44)H with N593(7.45)R, as well as D556(6.44)Q with either N593(7.45)R or N597(7.49)Q, produces average arrangements characterized by the absence of the Arg-442(3.50)-Asp-542(6.30) interaction, a feature of the active mutants, together with SAS below the threshold as in the inactive forms (Table IV, Fig. 4). Thus, molecular simulations suggest that the N593(7.45)R mutant antagonizes the solvent exposure of amino acids at the cytosolic extension of TMH 3 as triggered by the activating mutations of Asp-556(6.44) to His or Gln (Fig. 4). These results are consistent with the experimental findings that the D556(6.44)H/N593(7.45)R, D556(6.44)Q/N593(7.45)R, and D556(6.44)Q/N597(7.49)Q mutants are weakly or non-constitutively active (Table II).

In contrast, pairing D556(6.44)H with N597(7.49)Q retains all the features of the active mutants, the SAS index being similar to that of the D556(6.44)H single mutant (Fig. 4). This is consistent with the findings that the D556(6.44)H/N597(7.49)Q mutant is still constitutively active (Table II). Thus, the SAS values of the double mutants discussed above are significantly lower or, in one case only, similar to those of the highly active mutants, D556(6.44)H and D556(6.44)Q. Moreover, the double mutants show structural features that are not found in the single mutants, suggesting that the combined mutations influence each other. These result are consistent not only with the observed lack of additivity in the basal activity of these double mutants, but also with the antagonizing effect exerted by the Asn-593(7.45) and Asn-597(7.49) mutations on the constitutive activity of the D556(6.44)H and D556(6.44)Q mutants (Table III).

Finally, the model correctly predicts the triple mutants, D556(6.44)N/N593(7.45)A/N597(7.49)A and D556(6.44)H/N593(7.45)A/N597(7.49)A, as being non-constitutively active. In particular, pairing the N593(7.45)A mutant with the D556(6.44)H active mutant retains a SAS above the threshold, a feature of the active mutants, but associated with the presence of a weak Arg-442(3.50)-Asp-542(6.30) interaction. These results are consistent with the findings that the D556(6.44)H/N593(7.45)A mutant is still constitutively active (Table II). However, the additional mutation of Asn-597(7.49) to Ala, leading to the triple D556(6.44)H/N593(7.45)A/N597(7.49)A mutant, not only favors the Arg-442(3.50)-Asp-542(6.30) interac-

TABLE IV

Summary of results from molecular simulations on single, double, and triple mutants of LHR

The presence (+) or absence (−) of interactions between the side chains of amino acid residues at position 556 with 593 and at position 542 with 442 is indicated. NCA, non-constitutively active; CA, constitutively active, the latter given in boldface. Residues Arg-442, Asp-542, Asp-556, Asn-593, and Asn-597 correspond to (3.50), (6.30), (6.44), (7.45), and (7.49), respectively.

Mutant	556–593	442–542	SAS	Functionality
			$Å^2$	
WT	+	+	28	NCA
D542N[a]	+	+[c]	**93**	**CA**
D556H	−	−	**78**	**CA**
D556Q	+[b]	−	**86**	**CA**
D556A	−	−	**75**	**CA**
D556G[a]	−	+[c]	**111**	**CA**
D556Y[a]	+[c]	−	**100**	**CA**
D556L[a]	−	−	**65**	**CA**
D556N	+[c]	+[c]	29	NCA
N593R[d]	+	−	**43**	**CA**[d]
N597Q	+	−	**72**	**CA**
D542N/D556G[a]	+	+[c]	**61**	**CA**
D542N/D556Y[a]	+[c]	−	**91**	**CA**
D556H/N593A	−	+[c]	**75**	**CA**
D556H/N597Q	−	−	**79**	**CA**
D556H/N593R	+[c]	−	16	NCA
D556Q/N593R	+[c]	−	31	NCA
D556Q/N597Q	+[c]	−	36	NCA
D556N/N593D	+	−	2	NCA
D556N/N597D	+	+	25	NCA
D556H/N593A/N597A	−	+	31	NCA
D556N/N593A/N597A	−	+	43	NCA

[a] These mutants were described in Ref. 26.
[b] Different geometry.
[c] Weak interaction.
[d] Weakly CA.

tion but also abolishes completely the increase in solvent-accessible surface triggered by mutation of Asp-556(6.44) to His (Fig. 4). Overall, the results of simulations and experiments suggest that the breakage of the Asp-556(6.44)-Asn-593(7.45) H-bonding interaction is not sufficient to trigger constitutive LHR activation, but that LHR requires the conservation of both the Asn-593(7.45) and Asn-597(7.49) to be fully responsive to ligand. Indeed, non-conservative mutations of these amino acids may exert an "inhibitory" structural effect on the rearrangements of the cytosolic domains as promoted by activating mutations at Asp-556(6.44).

In summary, all the mutants engineered in this work induce perturbations, as compared with the wild type receptor, in the interaction pattern of the polar amino acids that are close to the mutated position or are the target of mutation. No clear correlation can be found between these structural changes in the proximity to the mutation site and the basal activity of the mutant. In contrast, perturbations in the interaction pattern of the highly conserved arginine of the (E/D)R(Y/W) sequence, as well as the solvent exposure of the cytosolic extensions of TMHs 3 and 6 (accounted for by the SAS index), that are far from the mutation site, nicely correlate with the constitutive activation of the mutant. In fact, highly constitutively active mutants are characterized by the absence of the charge reinforced H-bonding interaction between Arg-442(3.50) and Asp-542(6.30) and by SAS above the threshold, whereas the non-active mutants have associated SAS values below the threshold of 50 $Å^2$ and in some cases the presence of the Arg-442(3.50)-Asp-542(6.30) interaction. The weakly active mutants may show the co-existence of some features of the active forms and some others of the inactive ones.

It is noteworthy that the amino acid residues that participate in SAS do not contribute to the same extent in the different structures. Despite the fact that the differences in this index between inactive and active states are not that high, the threshold of 50 $Å^2$ properly differentiates the structures of the inactive forms from those of the active ones.

DISCUSSION

In this work, we have used experimental and computer-simulated mutagenesis to infer hypotheses on the molecular determinants for the susceptibility of Asp-556(6.44) to activating mutations and to gain insight into the structural features of mutation-induced active states of LHR. The presence of an aspartate in position (6.44) is a peculiarity of the glycoprotein hormone receptor subfamily. In fact, the majority of the GPCRs of the rhodopsin family share a phenylalanine in position (6.44), that is almost always paired with a tryptophan in position (6.48). In the α_{1b}-adrenergic receptor, Phe-303(6.44) has been found important for both agonist-stimulated receptor activation and susceptibility to activating mutations (35–37). Simulation and experiments on the α_{1b}-adrenergic receptor have suggested that Phe-303(6.44) lies in a position important for the transfer of information from the agonist binding site to the cytosolic portions of the helix 3-helix 6 interface (36, 37). The transduction of the structural change from the extracellular to the intracellular side of the α_{1b}-adrenergic receptor can be mediated by an aromatic cluster, including Phe-310(6.51), Trp-307(6.48), and Phe-303(6.44) (35–37). In LHR, the presence of an aspartate instead of phenylalanine is accompanied by an absence of both Trp(6.48) and Phe(6.51), consistent with the structural differences between the natural agonists of these two GPCRs. To probe the potential intramolecular interactions involving Asp-556(6.44), it has been mutated either alone or in combination with Asn-593(7.45) and Asn-597(7.49).

The results on single and double mutants of Asp-556(6.44), Asn-593(7.45), and Asn-597(7.49) indicate that both Asn-593(7.45) and Asn-597(7.49) are required for full constitutive activation of D556(6.44)H and D556(6.44)Q mutants. This hypothesis is strengthened by the fairly constant "loss" of constitutive activity, *i.e.* as viewed from additivity expectations (Table III), shown by double mutants of Asp-556(6.44)/Asn-593(7.45) and Asp-556(6.44)/Asn-597(7.49) that express at levels comparable with wild type LHR. The results obtained

with the two triple mutants of LHR, obtained by pairing a single mutant in TMH 6, either D556(6.44)H, which is constitutively active and ligand responsive, or D556(6.44)N, which exhibits characteristics like wild type LHR, with the double mutant in TMH 7, N593(7.45)A/N597(7.49)A, are also supportive of this interpretation.

Two of the most intriguing mutants examined herein are the reversals, D556(6.44)N/N593(7.45)D and D556(6.44)N/N597(7.49)D, comprising three constituent single LHR mutants, D556(6.44)N, N593(7.45)D, and N597(7.49)D, which exhibit rather different properties (this work and Ref. 23). Although the double mutants expressed at lower levels than wild type LHR, there is no evidence of constitutive activation in either of them. Moreover, they are less responsiveness to hCG than wild type LHR, perhaps attributable to some degree to the reduced expression. Phenotypically, these reversal mutants approximate the behavior of wild type LHR.

The rather complex findings from experimental mutagenesis have been complemented by molecular simulations on a molecular model of LHR based on the rhodopsin structure (4). The employed strategy essentially consisted of building a unique input structure for wild type LHR and its mutants that is capable of producing, following mutation and MD simulation, divergent structural effects for the active and the inactive forms. Once identified, the structural features responsible for this divergent behavior have been translated into theoretical descriptors, also useful for predicting the functional behavior of new LHR mutants. The employment of the same input structure for the wild type receptor and the mutant forms is an essential condition for evaluating the structural modifications induced by either non-activating or activating mutations as compared with the wild type receptor. In this comparative context, the input structure based upon the inactive state of rhodopsin has proven to be a valid approach for simulation of active and inactive LHR forms. Because studies have shown that constitutively active mutants of rhodopsin, *e.g.* E134(3.49)Q, adopt different orientations of helices 3 and 6 compared with that induced by photoactivation (38), even a photon-activated structure of rhodopsin would not necessarily provide a better starting structure for activating LHR mutants and would certainly not provide a tool for predicting the functional behavior of LHR mutants.

The model and SAS indices developed have proven successful in that the SAS indices obtained for wild type LHR also pertain to non-constitutively activating mutations and diverge significantly from those of activating mutations. Moreover, the model is capable of predicting the net effects of combining two and three functionally similar or different mutations (Figs. 2–4). The comparative analysis of the average structures derived from MD simulations of the wild type LHR, as well as of its naturally occurring activating and inactivating mutations, has been instrumental to infer the peculiar features differentiating the inactive from the active receptor states.[3]

Unique features of the wild type LHR within the homology model, as compared with the *ab initio* model previously proposed (6), are the charge-reinforced H-bonding interactions between Arg-442(3.50) and both the adjacent Glu-441(3.49) and Asp-542(6.30) in the cytosolic extension of TMH 6. This interaction pattern is associated with a solvent-accessible surface area computed over Arg-442(3.50), Thr-445(3.53), Ile-446(3.54), and Lys-541(6.29) (at the cytosolic extensions of TMHs 3 and 6) lower than 50 $Å^2$ (Fig. 2). Thus, according to the homology model, Asp-542(6.30) may contribute to stabilize the inactive state of the receptor through a charge-reinforced H-bonding interaction with the arginine of the (E/D)R(Y/W) sequence (Fig. 2). This hypothesis is supported by the experimental findings that substitutions of Asp-542(6.30) with Gly, Ala, Val, Leu, Phe, Lys, and Asn, that would break or weaken the interaction with Arg-442(3.50), result in constitutive activation, whereas substitution with glutamate does not (30, 39–41). The theoretical model suggests that the stabilizing effect of Asp-542(6.30) is more likely exerted via an interhelical salt bridge rather than via an intrahelix H-bonding interaction as very recently suggested (41). It is noteworthy that, in addition to rhodopsin, a salt bridge between the amino acids homologous to Arg-442(3.50) and Asp-542(6.30) in LHR has recently been suggested as one of the intramolecular constraints stabilizing the inactive states of the α_{1b}-adrenergic, β_2-adrenergic, and 5HT2A-serotoninergic receptors (37, 42–45).

Simulation of the activating mutation of Asp-542(6.30) to Gly produces average arrangements characterized by an augmented solvent exposure of Arg-442(3.50), as compared with wild type LHR, and consequently by SAS above the threshold (Fig. 2). These features of the active mutant persist over the 1-ns time of MD simulation. Similarly, the majority of the constitutively active mutants considered in this work are characterized by the breakage of the Arg-442(3.50)-Asp-542(6.30) charge-reinforced H-bonding interaction and by SAS values above the threshold. In contrast, the non-active mutants are characterized by the presence of the Arg-442(3.50)-Asp-542(6.30) interaction and by SAS below the threshold. Finally, weakly active mutants may display together some features of the inactive forms and some others of the active ones.

The theoretical SAS index computed on the double mutants engineered in this work is consistent with the observed lack of additivity in the basal receptor activity (Table III, Figs. 3 and 4). Moreover, consistent with the experimental findings, simulations predict that the combination of the D556(6.44)H or D556(6.44)Q active mutants with N593(7.45)R as well as of D556(6.44)Q with N597(7.49)Q is associated with a SAS index below the threshold, as in the inactive forms (Fig. 4). In contrast, combining N593(7.45)A or N597(7.49)Q with the active mutant D556(6.44)H results in a retention of the structural features of the active mutants.

Moreover, the model correctly predicts the antagonizing effect exerted by mutation of Asn-597(7.49) to Ala on the basal activity of the D556(6.44)H/N593(7.45)A active mutant. In fact, combining the D556(6.44)H mutant with N593(7.45)A to form the D556(6.44)H/N593(7.45)A double mutant, and with both N593(7.45)A and N597(7.49)A to form the D556(6.44)H/N593(7.45)A/N597(7.49)A triple mutant, progressively antagonizes the structural features of the active receptor forms found in the D566(6.44)H single mutant (Fig. 4). Thus, the degree of solvent exposure of the cytosolic extensions of TMHs 3 and 6 (SAS) appears to be a reliable indicator of whether LHR mutants will be constitutively active or not. These parameters presumably reflect access of crucial portions of LHR to the Gs protein.

In general, the average minimized structures of the double and triple mutants show structural peculiarities that cannot be found in the single mutants. This behavior is suggestive of a reciprocal influence of the effects exerted by co-existing mutations.

Our simulations strongly support the hypothesis that the Asp-556(6.44)-Asn-593(7.45) interaction is an important feature of wild type LHR. This interaction persists over the 1-ns time period of the equilibrated MD simulation and is retained in the reversal mutant D556(6.44)N/N593(7.45)D, consistent with the experimental finding that this mutant approximates the WT behavior. Positions 556(6.44) and 593(7.45) are, however, not equivalent. In fact, even if the D556(6.44)N/N593(7.45)D mutant retains the H-bonding interactions be-

tween the substituting residues, the wild type and the reversal mutant show structural differences between each other. Differences between these two LHR structures also concern the interaction patterns of the polar amino acids in TMHs 1, 2, 3, and 7. The non-equivalence of positions 556(6.44) and 593(7.45) is also suggested by the observation that the N593(7.45)A mutant is not constitutively active whereas D556(6.44)A is. The different structural/functional roles of Asp-556(6.44) and Asn-593(7.45) are also suggested by the fact that the former is a peculiarity of the glycoprotein hormone receptor subfamily, whereas the latter is highly conserved in the rhodopsin family of GPCRs.

Simulations suggest that the breakage of the Asp-556(6.44)-Asn-593(7.45) interaction in the D556(6.44)H/N593(7.45)A active mutant requires the integrity of Asn-597(7.49) to trigger the solvent exposure of the cytosolic extension of TMH 3. In fact, the Ala substituting for the Asn of the NP*XX*Y motif is able to antagonize the effect of the Asp-556(6.44) mutation. Indeed, this behavior may be a consequence of a strong connection between the highly conserved position and the cytosolic domains in the proximity to the arginine of the (E/D)R(Y/W) sequence. Overall, our results suggest that Asp-556(6.44) might play a role in stabilizing the inactive state of LHR, whereas Asn-593(7.45) and Asn-597(7.49) are required for the receptor to be fully responsive to ligand. However, the breakage or weakening of the Asp-556(6.44)-Asn-593(7.45) interaction is a peculiarity of the Asp-556(6.44) active mutants and, therefore, may be not required for ligand-induced LHR activation.

Molecular simulations and experiments based upon the use of single, double, and triple mutants of LHR have enabled us to probe likely interactions between certain amino acid residues and to demonstrate the pivotal role of TMHs 3, 6, and 7 in LHR function. Interestingly, two reports on TSHR recently appeared suggesting an important role of Asp-633(6.44) and Asn-674(7.49) in receptor activation (46, 47). Thus, Asp-Asn interactions between TMHs 6 and 7 appear to be extremely important in activation of the two homologous receptors, LHR and TSHR, although the results suggest that two distinct Asn residues, separated by about one helix turn in TMH 7, form the H-bond with Asp in TMH 6. These structural differences between LHR and TSHR concerning the interactions of the two conserved asparagines in TMH 7 are consistent with the observation that certain replacements of these amino acids give different functional effects in the two receptors (23, 47). Therefore, despite the high conservation of the two Asns and their environment, their preferential interaction patterns may not be exactly the same in the two glycoprotein-hormone receptors.

In conclusion, molecular simulations suggest that common features to the constitutively active LHR mutants are the breakage of the charge-reinforced H-bonding interaction between Arg-442(3.50) of the (E/D)R(Y/W) motif and Asp-542(6.30) and the increase in solvent accessibility of selected amino acids at the cytosolic extensions of TMHs 3 and 6. The conserved Asn-593(7.45) and Asn-597(7.49) in TMH 7 are structurally connected with these portions of the cytosolic domains as suggested by the finding that certain replacements of these amino acid residues antagonize the structural changes induced by activating mutations at Asp-556(6.44).

The SAS index accounting for these structural changes has proven to be a good predictor of the functional behavior of the LHR mutants, as well as the net effect of combining functionally similar or different mutants. The new models presented for wild type and mutant forms of LHR offer detailed insight into receptor function and can be used as a template for further mutagenesis studies.

Acknowledgments—It is a pleasure to thank Dr. Prema Narayan and Mr. Thomas Meehan for interest in the work, helpful suggestions, and assistance. We also thank Drs. Neil Bhowmick, Adrian Lapthorn, and J. Paul Simon for initial studies on molecular modeling and energy minimization of TMHs 6 and 7.

REFERENCES

1. Dufau, M. L. (1998) *Annu. Rev. Physiol.* **60,** 461–496
2. Fanelli, F., Themmen, A. P. N., and Puett, D. (2001) *IUBMB Life* **51,** 1–7
3. Segaloff, D. L., and, Ascoli, M. (1993) *Endocr. Rev.* **14,** 324–347
4. Palczewski, K., Kumasaka, T., Hori, T., Behnke, C. A., Motoshima, H., Fox, B. A., LeTrong, I., Teller, D. C., Okada, T., Stenkamp, R. E., Yamamoto, M., and Miyano, M. (2000) *Science* **289,** 739–745
5. Lin, Z., Shenker, A., and Pearlstein, R. (1997) *Protein Eng.* **10,** 501–510
6. Fanelli, F. (2000) *J. Mol. Biol.* **296,** 1333–1351
7. Baldwin, J. (1993) *EMBO J.* **12,** 1693–1703
8. Baldwin, J. M., Schertler, G. F., and Unger, V. M. (1997) *J. Mol. Biol.* **272,** 144–164
9. Unger, V. M., and Schertler, G. F. X. (1995) *Biophys. J.* **68,** 1776–1786
10. Unger, V. M., Hargrave, P. A., Baldwin, J. M., and Schertler, G. F. (1997) *Nature* **389,** 203–206
11. Braun, T., Schofield, P. R., and Sprengel, R. (1991) *EMBO J.* **10,** 1885–1890
12. Moyle, W. R., Campbell, R. K., Venkateswara Rao, S. N. Ayad, N. G. Bernard, M. P., Han, Y., and Wang, Y. (1995) *J. Biol. Chem.* **270**, 20020–20031
13. Kajava, A. V., Vassart, G., and Wodak, S. J. (1995) *Structure* **3,** 867–877
14. Jiang, X., Dreano, M., Buckler, D. R., Cheng, S., Ythier, A., Wu, H., Hendrickson, W. A., and El Tayar, N. (1995) *Structure* **3,** 1341–1353
15. Bhowmick, N., Huang, J., Puett, D., Isaacs, N. W., and Lapthorn, A. J. (1996) *Mol. Endocrinol.* **10,** 1147–1159
16. Couture, L., Naharisoa, H., Grebert, D., Remy, J.-J., Pajot-Augy, E., Bozon, V., Haertle, T., and Salesse, R. (1996) *J. Mol. Endocrinol.* **16,** 15–25
17. Kobe, B., and Deisenhofer, J. (1993) *Nature* **366,** 751–756
18. Shenker, A. (1998) in *Contemporary Endocrinology: G Proteins, Receptors and Disease* (Spiegel, A. M., ed) pp. 139–152, Humana Press, Inc., Totowa, NJ
19. Chan, W.-Y. (1998) *Mol. Genet. Metab.* **63,** 75–84
20. Themmen, A. P. N., Martens, J. W. M., and Brunner, H. G. (1998) *Mol. Cell. Endocrinol.* **145,** 137–142
21. Latronico, A. C., and Segaloff, D. L. (1999) *Am. J. Human Gen.* **65,** 949–958
22. Ballesteros, J. A., and Weinstein, H. (1995) *Methods Neurosci.* **25,** 366–428
23. Angelova, K., Narayan, P., Simon, J. P., and Puett, D. (2000) *Mol. Endocrinol.* **14,** 459–471
24. Kosugi, S., Lin, Z., Pearlstein, R., Mori, T., and Shenker, A. (1997) *Abstracts of the 79th Annual Meeting of the Endocrine Society, Minneapolis, June 11–14, 1997*, p. 171 (abstr.)
25. Fernandez, L. M., and Puett, D. (1996) *Biochemistry* **35,** 3986–3993
26. Kosugi, S., Mori, T., and Shenker, A. (1996) *J. Biol. Chem.* **271,** 31813–31817
27. Laue, L. L., Wu, S.-M., Kudo, M., Bourdony, C. J., Cutler, G. B., Jr., Hsueh, A. J. W., and Chan, W.-Y. (1996) *Mol. Endocrinol.* **10,** 987–997
28. Latronico, A. C., Anasti, J., Arnhold, I. J. P., Rapoport, R., Mendonca, B. B., Bloise, W., Castro, M., Tsigos, C., and Chrousos, G. P. (1996) *New Engl. J. Med.* **334,** 507–512
29. Kraaij, R., Post, M., Kremer, H., Milgrom, E., Epping, W., Brunner, H. G., Grootegoed, J. A., and Themmen, A. P. N. (1995) *J. Clin. Endocrinol. Metab.* **80,** 3168–3172
30. Kosugi, S., Mori, T., and Shenker, A. (1998) *Mol. Pharmacol.* **53,** 894–901
31. Sali, A., and Blundell, T. L. (1993) *J. Mol. Biol.* **234,** 779–815
32. Brooks, B. R., Bruccoleri, R. E., Olafson, B. D., States, D. J., Swaminathan, S., and Karplus, M. (1983) *J. Comput. Chem.* **4,** 187–217
33. Liu, G., Duranteau, L., Carel, J.-C., Monroe, J., Doyle, D. A., and Shenker, A. (1999) *New Engl. J. Med.* **341,** 1731–1736
34. Simon, J. P., Angelova, K., and Puett, D. (2002) *Protein Pept. Lett.* **9,** 153–158
35. Chen, S., Xu, M., Lin, F., Lee, D., Riek, P., and Graham, R. M. (1999) *J. Biol. Chem.* **274,** 16320–16330
36. Chen, S., Lin, F., Xu, M., and Graham, R. M. (2002) *Biochemistry* **42,** 588–596
37. Greasley, P. J., Fanelli, F., Rossier, O., Abuin, L., and Cotecchia, S. (2002) *Mol. Pharmacol.* **61,** 1025–1032
38. Kim, J. M., Altenbach, C., Thurmond, R. L., Khorana, H. G., and Hubbell, W. L. (1997) *Proc. Natl. Acad. Sci. U. S. A.* **94,** 14273–14278
39. Schulz, A., Schöneberg, T., Paschke, R., Schultz, G., and Gudermann, T. (1999) *Mol. Endocrinol.* **13,** 181–190
40. Schoneberg, T., Schultz, G., and Gudermann, T. (1999) *Mol. Cell. Endocrinol.* **151,** 181–193
41. Schulz, A., Bruns, K., Henklein, P., Krause, G., Schubert, M., Gudermann, T., Wray, V., Schultz, G., and Schoneberg, T. (2000) *J. Biol. Chem.* **275,** 37860–37869
42. Greasley, P. J., Fanelli, F., Scheer, A., Abuin, L., Nenniger-Tosato, M., DeBenedetti, P. G., and Cotecchia, S. (2001) *J. Biol. Chem.* **276,** 46485–46494
43. Ballesteros, J. A., Jensen, A. D., Liapakis, G., Rasmussen, S. G. F., Shi, L., Gether, U., and Javitech, J. A. (2001) *J. Biol. Chem.* **276,** 29171–29177
44. Shapiro, D. A., Kristiansen, K., Weiner, D. M., Kroeze, W. K., and Roth, B. (2002) *J. Biol. Chem.* **277,** 11441–11449
45. Visiers, I., Ebersole, B., Dracheva, S., Ballesteros, J., Sealfon, S. C., and Weinstein, H. (2002) *Int. J. Quant. Chem.* **88,** 65–75
46. Govaerts, C., Lefort, A., Costagliola, S., Wodak, S. J., Ballesteros, J. A., Van Sande, J., Pardo, L., and Vassart, G. (2001) *J. Biol. Chem.* **276,** 22991–22999
47. Neumann, S., Krause, G., Chey, S., and Paschke, R. (2001) *Mol. Endocrinol.* **15,** 1294–1305